ANNUAL REPORT 2005

Meeting date: June 1, 2005

Study on Hook Formation in Ultra-low Carbon Steel Slabs

Joydeep Sengupta
Postdoctoral Research Associate
& Brian G. Thomas

Department of Mechanical & Industrial Engineering
University of Illinois at Urbana-Champaign

Types of oscillation marks

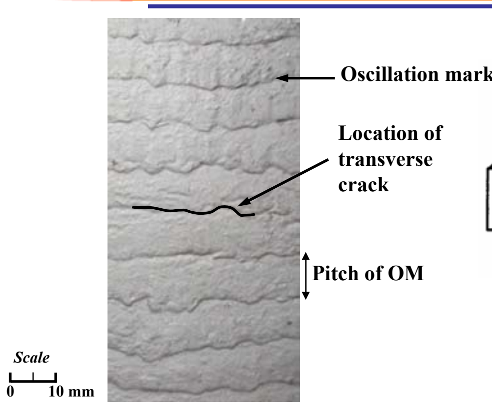

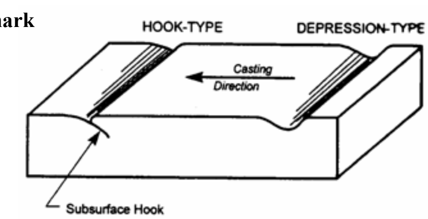

Szekeres, Iron & SteelMaker, 1996

Hook-type OMs are generally deeper and can be distinguished visually

POSCO casting trials on ultra-low carbon slabs (2004):

- **Typical OM depth = ~0.2 – 0.6 mm**
- **OMs with hooks > 98% on narrow face for different casting conditions (12 out of 13)**
  = 100% on wide face (7 out of 10) – 70-90% (3 out of 10)

Types of hook marks (ultra-low carbon steel)

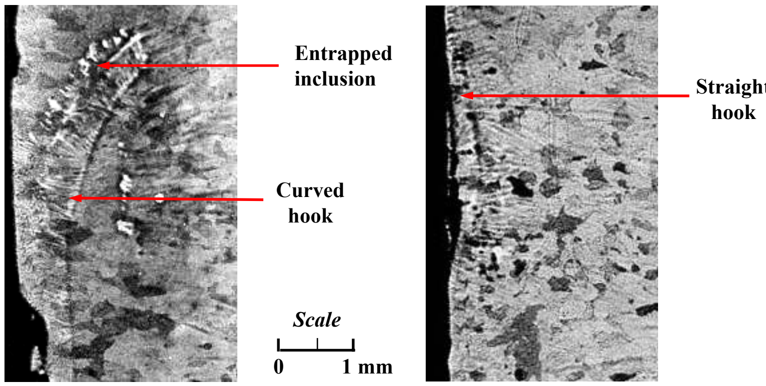

- ~20-35% straight hooks (wide + narrow faces) based on 13 POSCO trials in 2004
- OMs with curved hooks are generally deeper (~1.5 times)
- Scarfing is usually done to remove hooks & related defects

OM/Hook formation more severe with decreasing carbon content

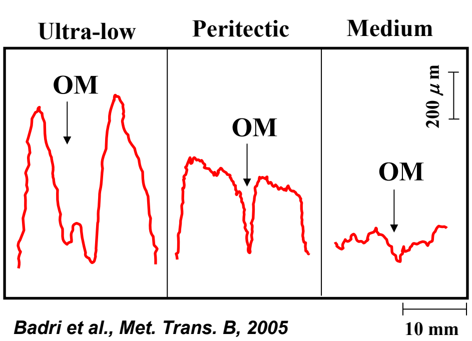

Badri et al., Met. Trans. B, 2005

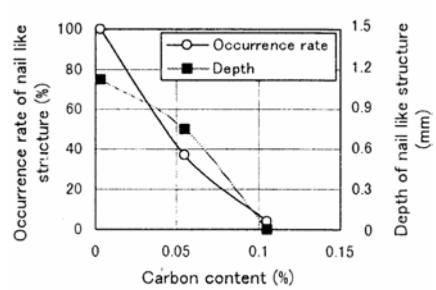

Suzuki, CAMP-ISIJ, 1998

- Ultra-low carbon steels have deeper OMs and are more prone to form hooks
- Higher solidus (1535 °C ↔ 1500 °C for high carbon steels) & thinner mushy zone (15 °C ↔ 50 °C for high carbon steels)

OM/Hook formation in meniscus region

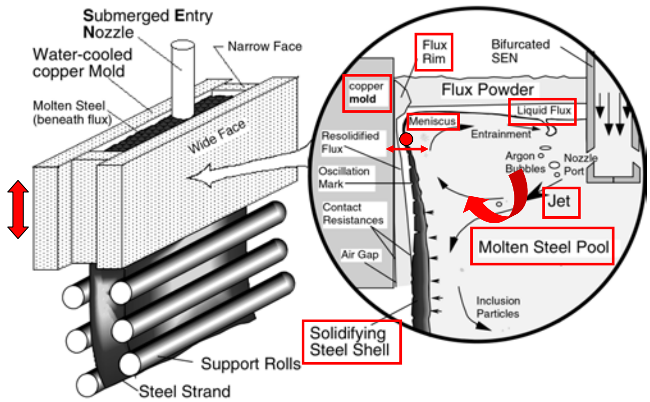

- **Combined effect of heat transfer, solidification, mechanical interactions & fluid flow**
- **Meniscus region: extends to ~10 mm below the metal level**
- **Influencing events last for a very short time-span but occurs periodically**

Influential event #1

Heat transfer between shell and mold:

Heat is conducted into the mold via liquid flux & re-solidified flux layers
- **Governed by size & properties of interfacial gap (contact resistance)**
- **Dynamic mold distortion can lower contact resistance locally**

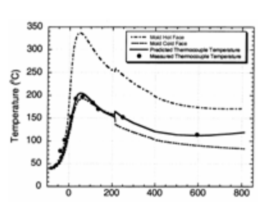

Meng and Thomas, Met. Trans. B, 2004

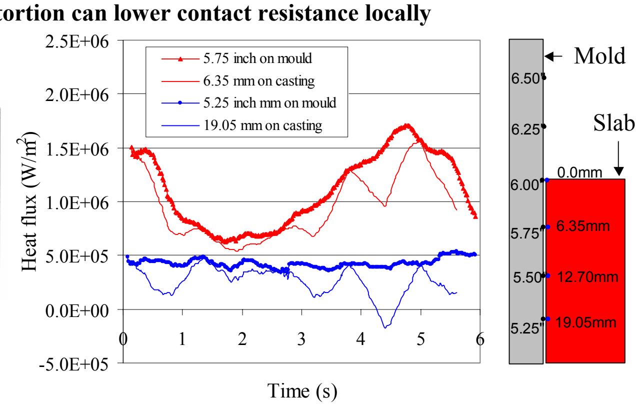

Li and Thomas, Private Communication, 2005

Periodic rise in heat flux near meniscus

Rise in heat flux attributed to release of latent heat (meniscus freezing)

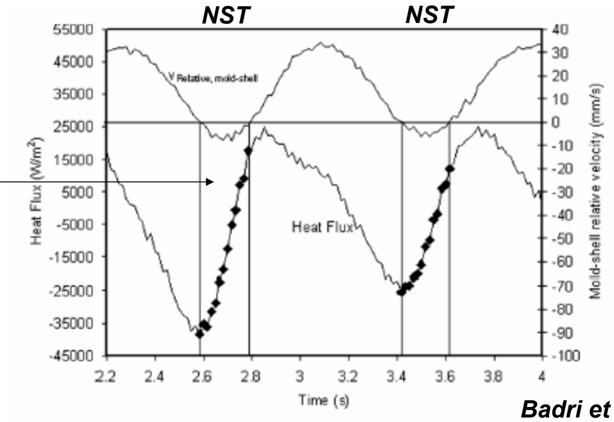

Badri et al., Met. Trans. B, 2005

Measurements for ulta-low carbon steel in a laboratory scale simulator at CMU

Link between periodic rise in heat transfer & OM formation

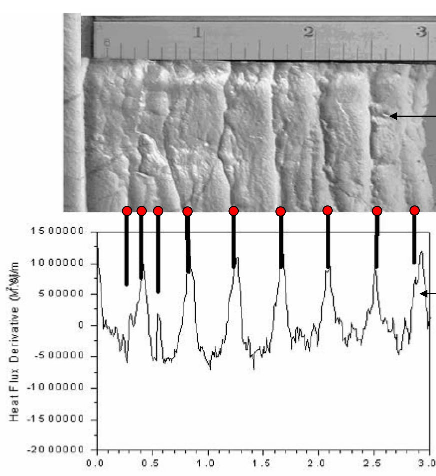

Oscillation marks on a ultra-low carbon steel slab

Periodic rise in heat flux during NST

Badri et al., Met. Trans. B, 2005

Measurements for ulta-low carbon steel in a laboratory scale simulator at CMU

Influential event #2

Meniscus shape:

- **Shape determined by balance of surface tension, pressure & gravity forces (equilibrium shape can be predicted by Bikerman's equation)**
- **Strong function of sulfur content of steel**
- **Pressure forces due to mold oscillation is transmitted to meniscus via flux layer (both temporal & spatial variations)**

Equilibrium meniscus shape

$$x - x_0 = -\sqrt{2a^2 - z^2} + \frac{a}{\sqrt{2}} ln \frac{a\sqrt{2} + \sqrt{2a^2 - z^2}}{z}$$

$$x_0 = a - \frac{a}{\sqrt{2}} ln(\sqrt{2} + 1)$$

$$a = \sqrt{\frac{2\gamma}{\rho_{steel} g}}$$

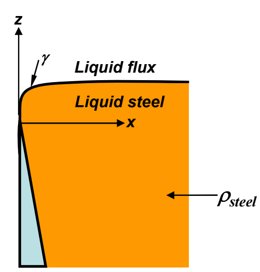

x = distance perpendicular to the mold wall in mm
Z = distance along the mold wall in mm
γ = surface tension between liquid steel and vapor (or flux) in N m^{-1}
ρ_{steel} = density of liquid steel = 7000 kg m^{-3}
g = gravitational acceleration = 9.81 m s^{-2}

From Bikerman, Physical Surfaces, Academic Press, 1970

Effect of %S on surface tension

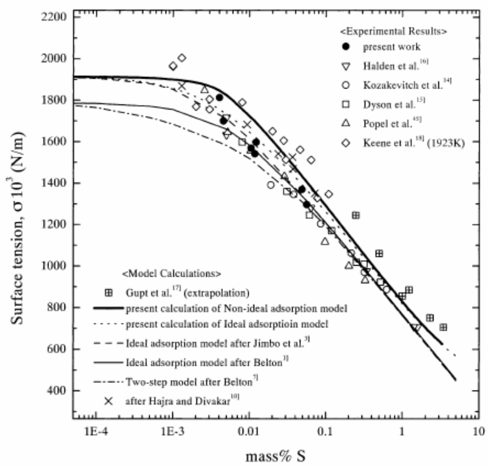

Lee and Morita, ISIJ International, 2002

Meniscus shape – affected by sulfur content

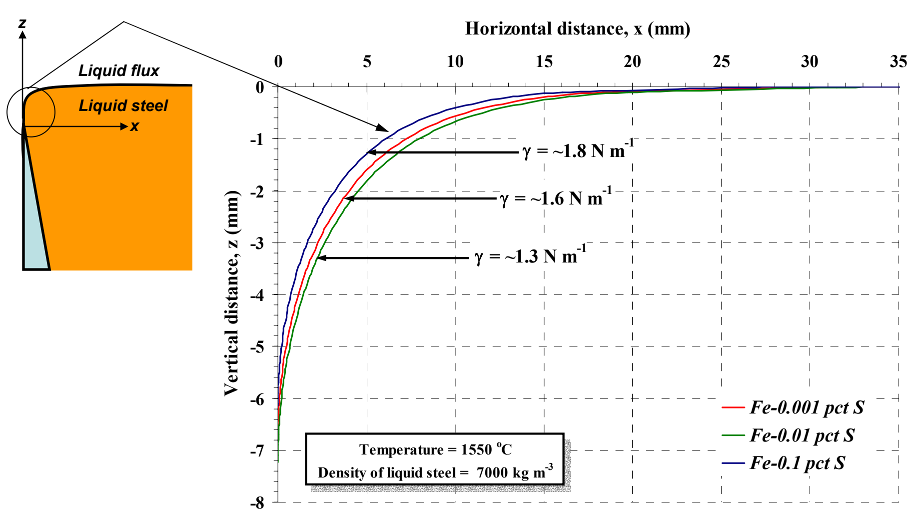

Dynamic flow effects at meniscus (due to mold oscillation)

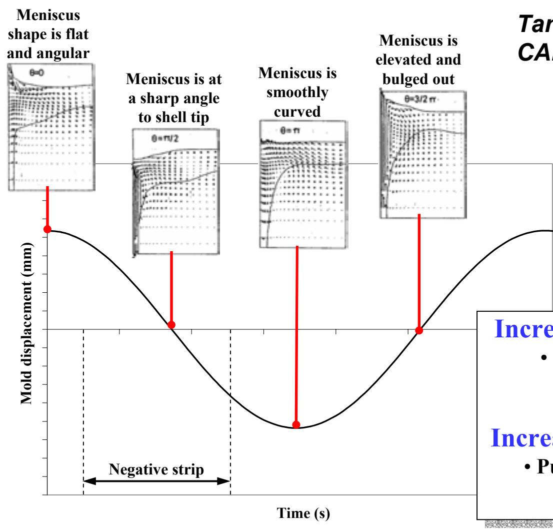

Tanaka and Takatani, CAMP-ISIJ, 1989

Increasing positive flux pressure:
- **Brings meniscus close to mold**
- **Facilitates sudden freezing**

Increasing negative flux pressure:
- **Pushes meniscus away from mold**
- **Meniscus Bulging**

Influential event #3

Meniscus Freezing:

Partial solidification of meniscus can occur in presence of a water-cooled mold *(Saucedo, 1991)*

- **Preservation of instanteneous frozen shape**
- **Rapid cell growth in the presence of under-cooled liquid (heterogeneous nucleation)**
- **Incorporated into OM mechanisms (Takeuchi & Brimacombe in 1984)**

©

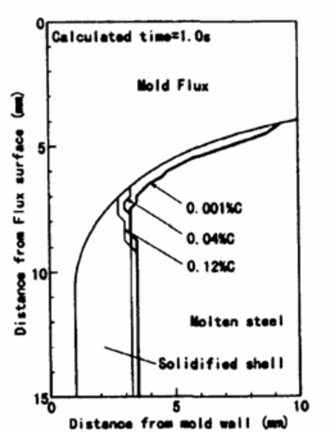

Yamamura et al., ISIJ International, 1996

Influential event #4

Fluid flow effects:

- Steel jets perturb free surface (standing waves)
- Level fluctuations due to chaotic turbulence & presence of particles/bubbles (buoyancy forces)
- Abrupt changes in operating conditions (e.g. release of nozzle clog)

Local level fluctuations

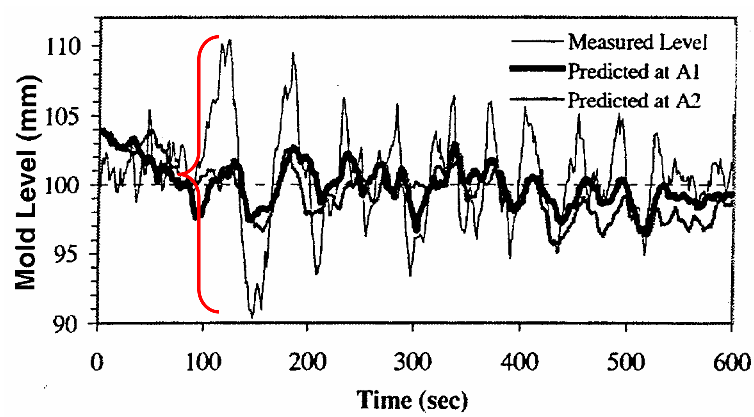

Lai et al., ISS Steelmaking Conference, 2000

Influential event #5

Delivery of local superheat:

- Distributed via metal jets & follows the fluid flow patterns to reach meniscus
- Meniscus typically retains ~30% of total superheat available (no freezing)

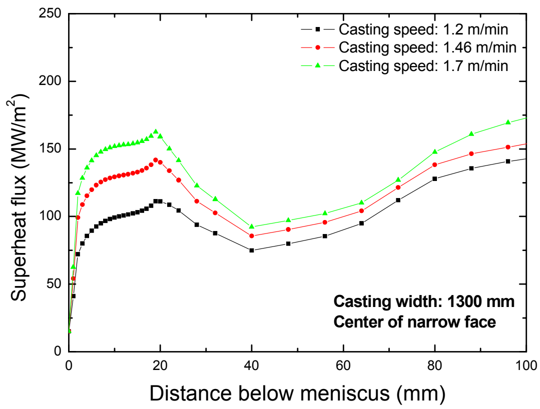

Zhang and Thomas, POSCO Report, 2004

Influential event #6

Shell tip deformation:

Shell tip may move away or towards the mold surface due to thermal stresses (temperature gradients) and/or mechanical effects

- **Solidification mode (large shrinkage is associated with $\delta \rightarrow \gamma$ transformation)**
- **Local shell thinning due to presence of air gap & OMs (coupled effect)**
- **Mechanical interaction between shell tip and solid rim (negative strip period)**
- **Sticking of shell tip to mold wall in absence of flux (hot tearing)**
- **Sudden level fluctuation exposing shell interior to flux**

Level drop effect: shell bending

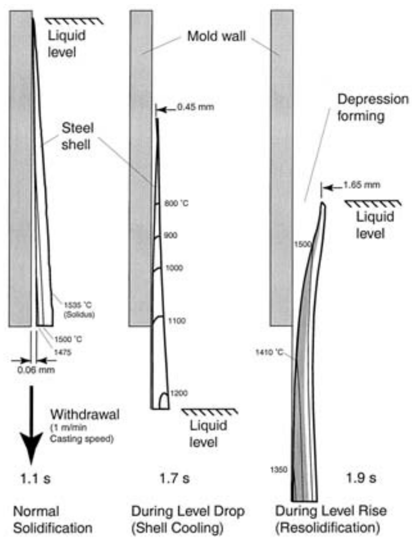

- *During level drop:*
  Shell interior exposed to flux
  Left edge of shell cools rapidly
  Shell tip bends away from mold
- *After level rise:*
  New shell forms on existing solid
  Bending of shell increased further

B.G. Thomas and H. Zhu, Solidification Science & Processing Conference, 1996

OM formation mechanism I

Steel solidifies first against mold wall forming a secondary meniscus & attaches to shell during negative strip time

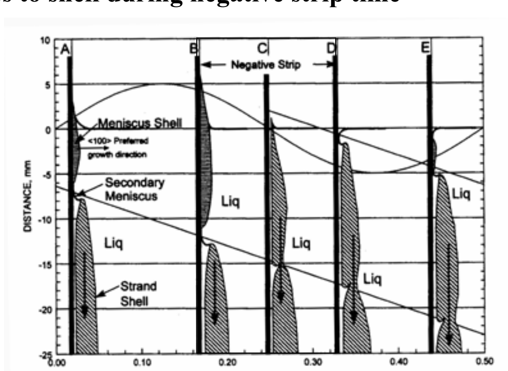

Healing: (i) Sato (Proc. of NOH & BOS Conf.), 1979
(ii) Szekeres (Iron & Steel Engineer), 1996
Tearing: Savage and Pritchard (Iron and Steel), 1954

OM formation mechanism II

Shell distortion (away from mold) & subsequent overflow

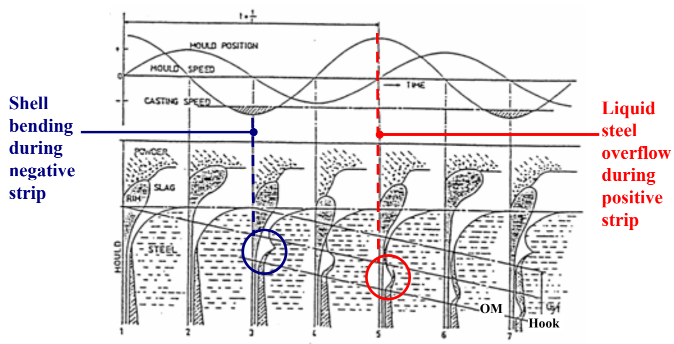

(i) Schwerdtfeger and Sha (Met. Trans. B), 2000: *Beam bending theory*
(ii) Thomas and Zhu, 1996: *Level drop causes surface depressions*
(iii) Emi *et al.* (Proc. of NOH & BOS Conf.), 1978: *Solid flux rim effect*

OM formation mechanism III

Meniscus freezing & subsequent overflow

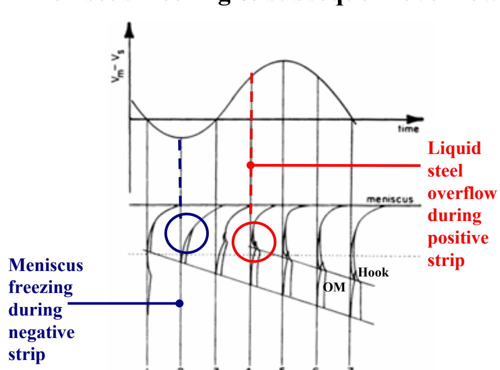

(i) Takeuchi and Brimacombe (Met. Trans. B), 1984: *Metallography*
(ii) Saucedo (SteelMaking Conf. Proc.), 1991: *Metallography*
(iii) Putz *et al.* (Steel Research), 2003: *Heat transfer/Fluid flow model*

Two mechanisms for hook formation have been considered in this study

I. Solidification of curved liquid steel meniscus

II. Solidification of steel shell against the mold wall and then subsequent distortion due to thermal stress / pressure forces

Re-evaluate mechanisms by:
- Analysis of hook metallography (POSCO/Postech)
- EBSD analysis of hooks
- Meniscus shape calculation
    - Thermal-stress analysis of initial solidification

Propose new mechanism of hook formation

Hook characteristics

Hook depth, D = 1.82 mm
Hook height, H = 5.37 mm
Hook length, L = 5.65 mm
Hook thickness, T = 0.78 mm
OM depth, d = 0.228 mm
Final hook angle, $\theta = 69^{o}$

Ultra low carbon steel (0.003% C)
POSCO Sample No.:
B58077-02-2 No.1-1 (Curved hook)

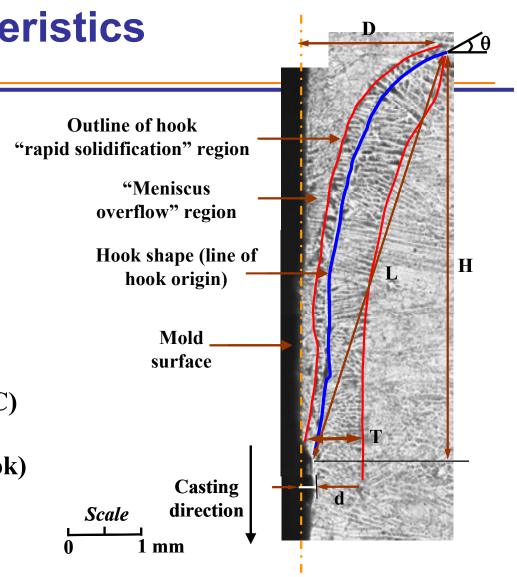

Hook shapes: *Case I*

Ultra low carbon steel:
0.003C-0.009S-0.08Mn-0.013P-0.039Al-0.047Ti-0.01Ni-0.01Cr-0.01Cu

Casting conditions:
Casting speed : 1.42 m/min
Frequency: 155 cpm
Stroke: 6.34 mm
Superheat: 25 °C

POSCO Casting No.: B58077-02
Samples taken within ~100mm of slab length

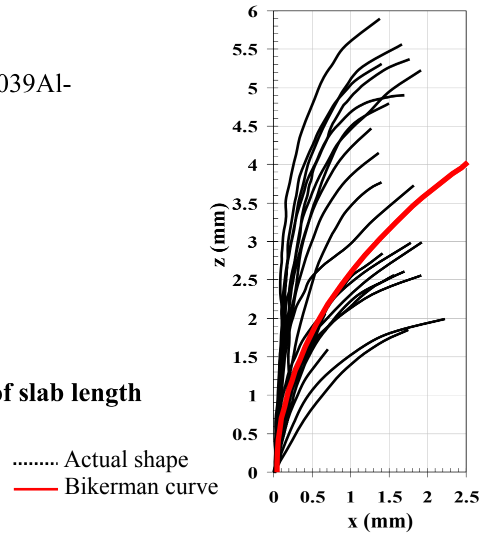

Hook shapes: *Case II*

Ultra low carbon steel:
0.003C-0.009S-0.08Mn-0.013P-0.039Al-0.047Ti-0.01Ni-0.01Cr-0.01Cu

Casting conditions:
Casting speed : 1.61 m/min
Frequency: 181 cpm
Stroke: 6.82 mm
Superheat: 27 °C

POSCO Casting No.: B58075-06
Samples taken within ~100mm of slab length

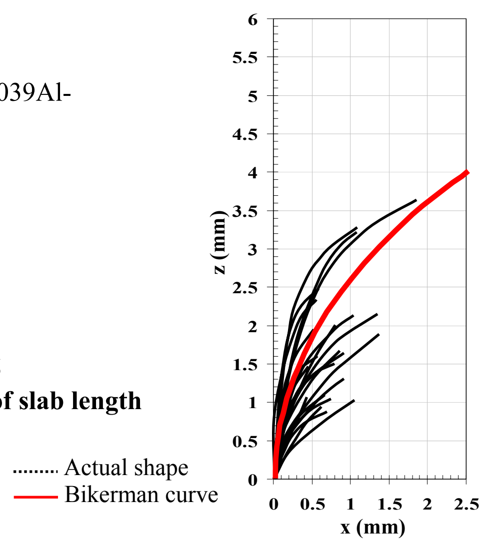

Variations in hook angle, and meniscus shape before & after "meniscus overflow"

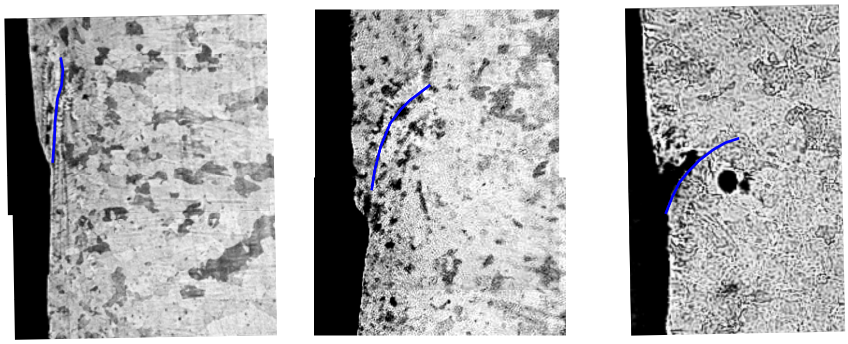

(a) **(b)** **(c)**

Different shapes of meniscus: (a) almost straight to (c) very bent
Different shapes of overflow region: (a) shallow contact angle, (b) near-vertical contact angle, & (c) strange angle and shape

Hooks with particles showing capture before and after "meniscus overflow"

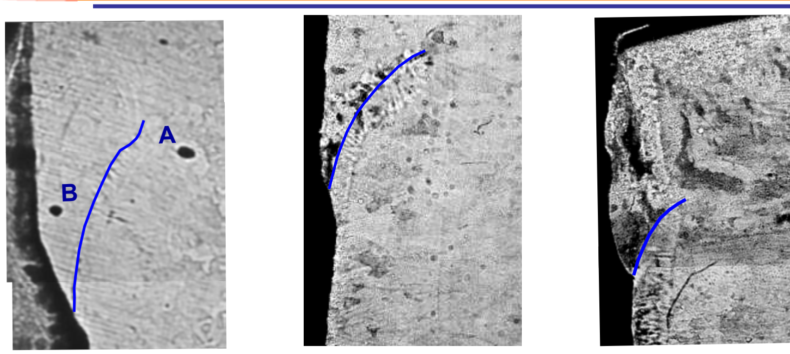

Bubble A entrapped by frozen meniscus *but*
Bubble B flows along with the overflowing liquid steel

Debris trapped on both sides of the line of hook origin:

Below the line of hook origin: particles flow up with the steel, reach the meniscus, *but do not get entrained into slag layer*

Above the line of hook origin: particles flow along with the overflowing liquid steel *when it overflows the meniscus*

Features of a hook tip

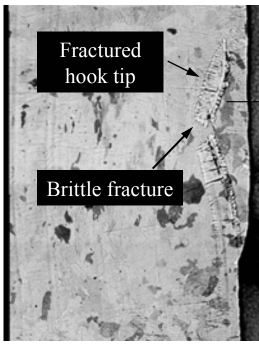

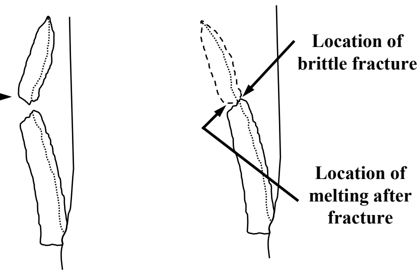

Actual position of hook and fractured tip on slab

Original position of fractured tip prior to brittle fracture

Truncated hooks

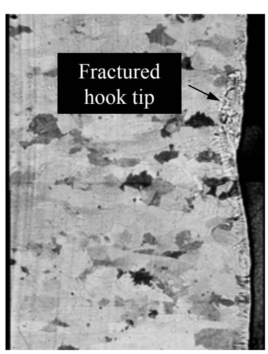

Truncated hook and unmelted fractured tip

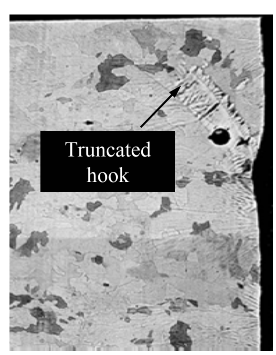

Truncated hook (Fractured tip melted away)

Cell growth near hook

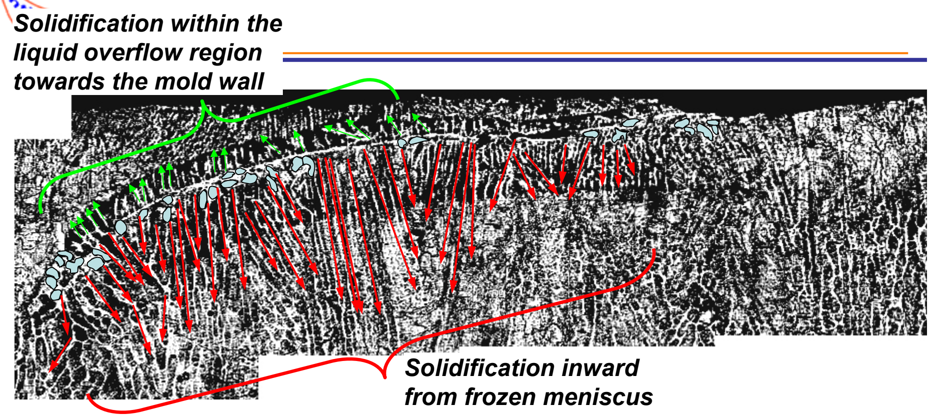

- Random orientation of dendrites → *Heterogeneous nucleation*
- Fine dendrite arms near origin line → *rapid solidification of undercooled liquid*
- Coarser dendrite arms → *Lower temperature gradient*
  → long time surrounded by liquid before solidification continued (ripening)
- Large sudden change of growth direction → *Movement of fractured hook tip*

SEM Images

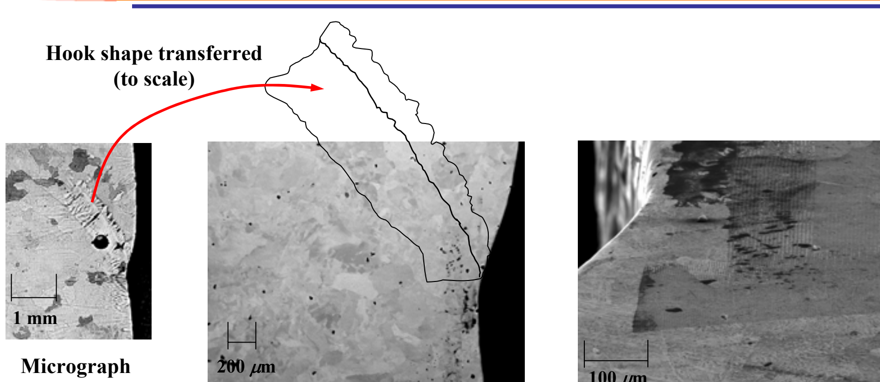

Micrograph from optical microscope

Backscattered SEM image

Backscattered SEM image with 70 degrees tilt

Electron Back Scattered Diffraction (EBSD) Map near hook region

Grains can be identified on the sample by superimposing an EBSD map containing grain orientation information on the Backscattered SEM image

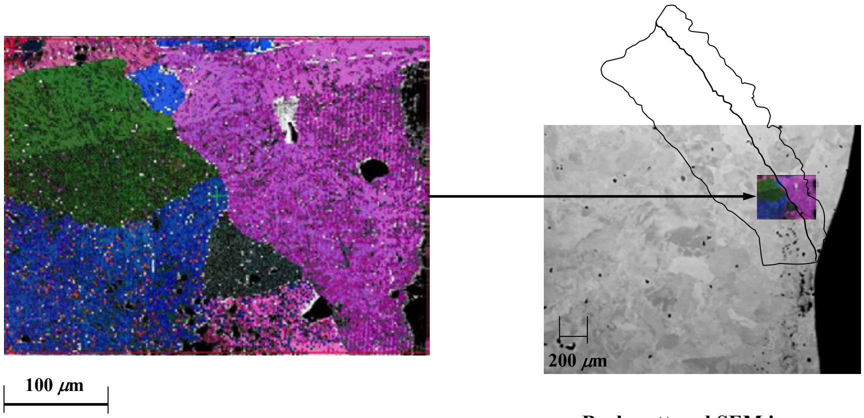

Backscattered SEM image

Quantification of grain misorientation

EBSD postprocessor software can provide local grain misorientation data

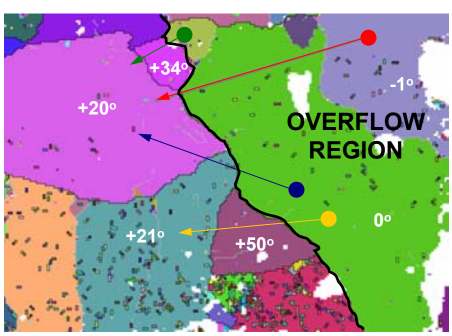

100 μm

300x

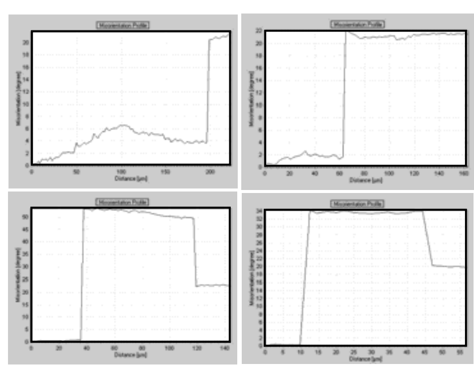

Location of line of hook origin on EBSD image compares well with micrograph

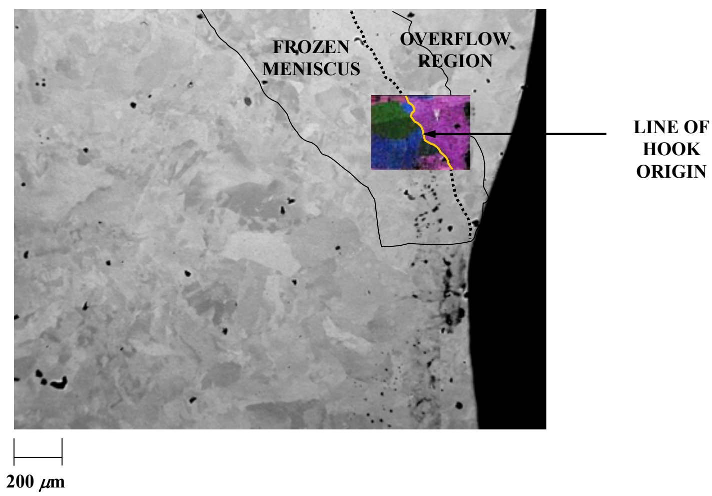

CON2D Finite-element model to compute thermal distortion of solidifying steel shell

Simulation Details

- Domain Size: 3 mm x 30 mm
- 6 noded triangular elements
- Mesh resolution: 0.1 mm x 0.5 mm

Assumptions:

- Effect of ferrostatic pressure is ignored
- No constraint at the mold edge
- No mold taper, slag, oscillation, friction
- Drop in heat transfer due to air gap ignored
- Level is assumed to drop suddenly
- No kinetics & undercooling effects

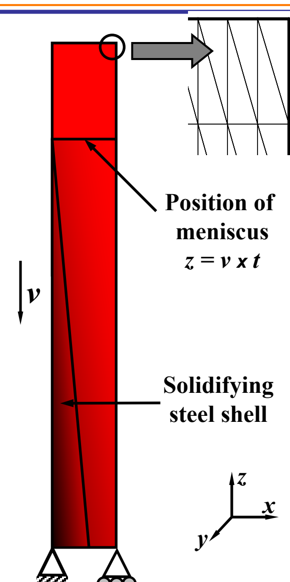

Simulation conditions

Grade	Ultra-low C steel
Composition	0.003C-0.009S-0.08Mn-0.013P-0.039Al-0.047Ti-0.01Ni-0.01Cr-0.01Cu
$T_{solidus}$	1519.3 °C
$T_{liquidus}$	1533.9 °C
ΔT	14.6 °C
$\Delta T_{superheat}$	30 °C
Casting speed	1.2 m/min
T_{mold}	250 °C
T_{flux}	1000 °C
Sudden level drop at	0.8 s (for 16, 8, 5 & 3 mm)
Sudden level rise at	1.2 s
Total time for analysis	1.5 s (0.001 s time step size)

Phase fractions

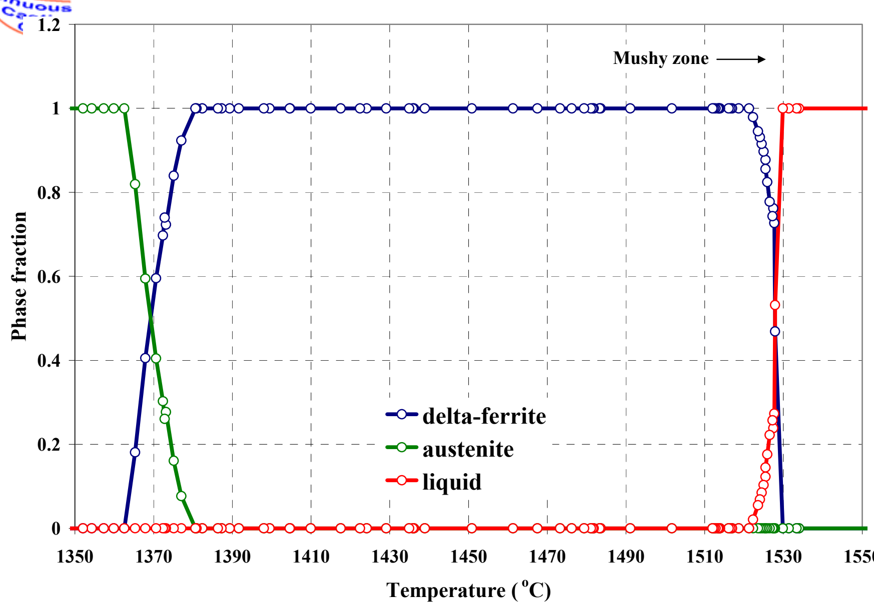

Thermophysical properties

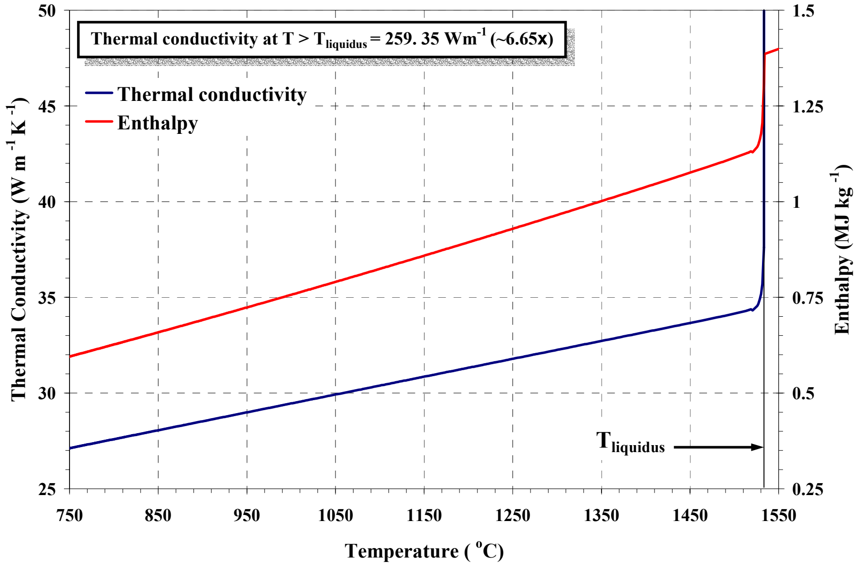

Mechanical properties

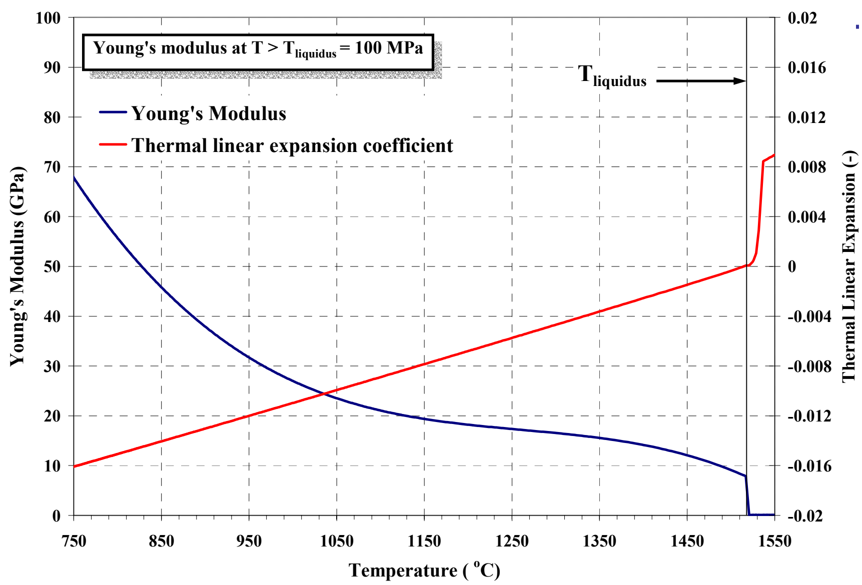

Constitutive behavior

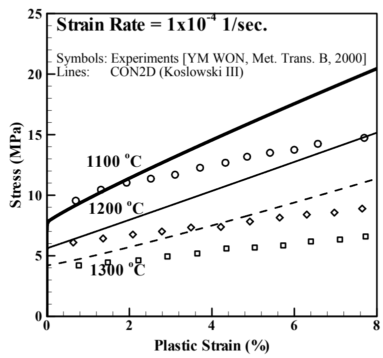

Kozlowski III Law for Austenite

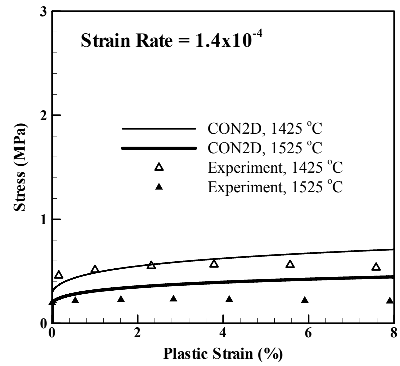

Power Law for δ-ferrite

Heat Transfer Calculations

Level fluctuation history

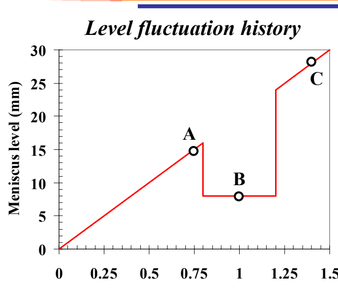

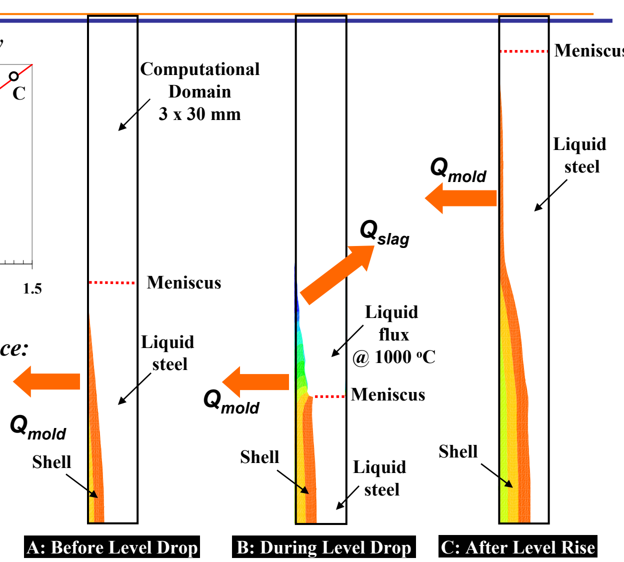

Mold - solidifying shell interface:

$Q_{mold} = h_{mold}$ x $(T_{shell} - 250)$

$h_{mold} = 4000$ Wm^2K^{-1}

Slag – shell interface:

$Q_{slag} = h_{slag}$ x $(T_{shell} - T_{slag})$

$h_{slag} = 2300$ Wm^2K^{-1}

$T_{slag} = 1000$ °C

Shell deformation during level fluctuation

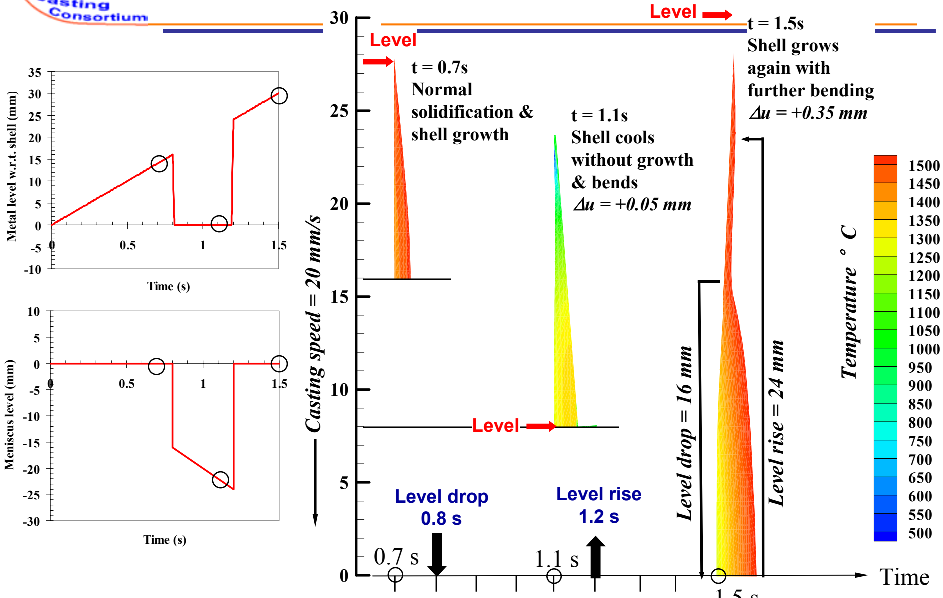

Final distorted shape for different level drop distances (0.3s after overflow over shell tip)

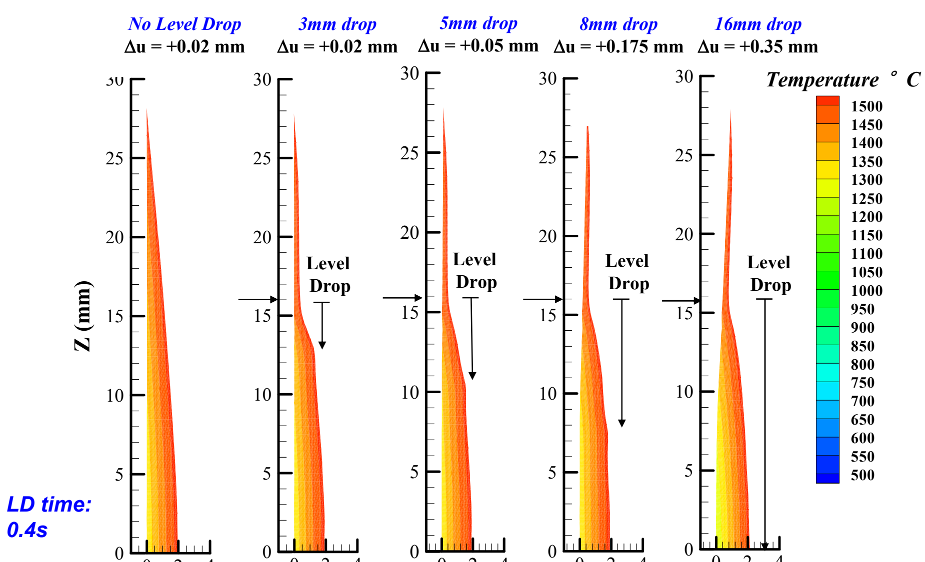

Jog formation

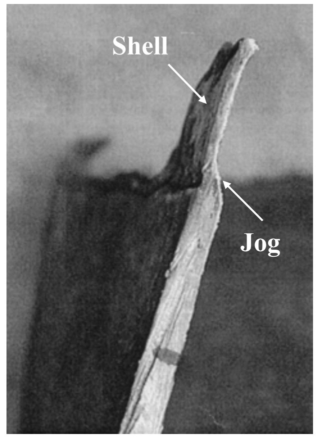

Fredriksson and Elfsberg, Scandinavian J. of Met., 2002

Comparison between hook and distorted shell shapes

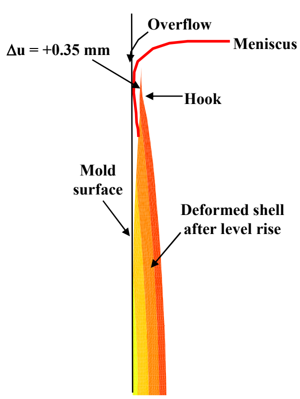

Mechanism of hook formation due to shell distortion associated with a level drop event

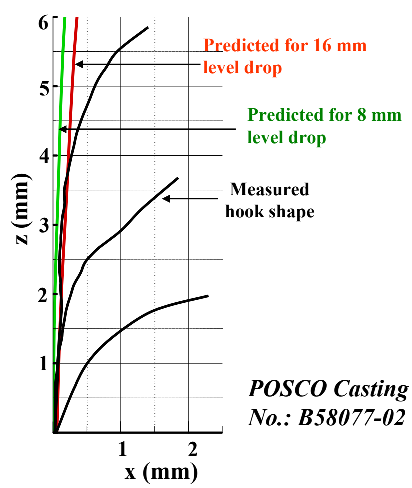

Shell distortion will affect OM & hook formation during large level drops

Hook depth measured from POSCO samples (2004 data)

Sample	OM #	Hook #	Surface hook #	Curved hook #	% Surface hooks	% Curved hooks	Mean hook depth (mm)	Max hook depth (mm)	Min hook depth (mm)
B32793-02	49	48	11	37	22.9	77.1	0.83	1.53	0.39
B32793-05	49	47	9	38	19.1	80.9	0.83	1.30	0.44
B32793-52	62	61	15	46	24.6	75.4	0.73	1.60	0.29
B31075-04	*51*	*44*	*19*	*25*	*43.2*	*56.8*	*0.77*	*1.49*	*0.34*
B31075-05	48	47	14	33	29.8	70.2	1.11	1.83	0.38
B31077-04	52	51	9	42	17.6	82.4	1.06	1.92	0.47
B31077-54	48	48	11	37	22.9	77.1	0.96	2.10	0.21
B26848-04	27	27	3	24	11.1	88.9	1.09	2.05	0.62
B26848-54	26	26	9	17	34.6	65.4	1.03	1.58	0.52
B30957-01	55	53	17	35	32.7	67.3	1.12	3.21	0.53
B30959-02	48	48	19	29	39.6	60.4	1.05	1.91	0.42
B30959-51	*51*	*51*	*20*	*32*	*38.5*	*61.5*	*1.79*	*3.21*	*0.55*
B30959-55	*51*	*50*	*22*	*28*	*44.0*	*56.0*	*1.60*	*2.61*	*0.53*

Proposed mechanism for hook formation

HOOK FORMATION

Mechanism:
Meniscus freezing & Liquid overflow in the presence of uncooled liquid during negative strip time

⇩

CURVED HOOK

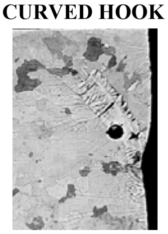

Mechanism:
Shell distortion during negative strip time

⇩

STRAIGHT HOOK

Development of a detailed hook formation mechanism

• Events dictating formation of OMs and hooks are complex, inter-dependent and transient

• Plant experiments cannot reveal detailed steps that lead to final microstructure and morphology

• Development of a comprehensive computational model is a daunting task

• *Alternative methodology:*
- Combine existing modeling results & plant observations
- Construct a series of schematics illustrating the mechanism
- Will not predict formation of hooks, but will lead to model development

Three hooks observed on a POSCO slab

I. Steel Composition:
C (0.003%) - **Mn** (0.08%) - **Si** (0.005%) - **P** (0.015%) – **S** (0.01%) - **Cr** (0.01%) - **Ni** (0.01%) - **Cu** (0.01%) – **Ti** (0.05%) - **Al** (0.04%)

II. Steel Properties:	
Liquidus temperature (in °C):	1533
Solidus temperature (in °C):	1517
Density of liquid steel (in kg m^{-3}):	7000
Surface tension at 1550 °C (in N m^{-1}):	1.6
III. Slag Properties:	
Solidification temperature (in °C):	1149
Melting temperature (in °C):	1180
Viscosity at 1300 °C (in Poise):	3.21
IV. Casting conditions:	
Casting speed:	1.394 m min^{-1}
Frequency of mold oscillation:	174 cpm
Stroke of mold oscillation:	5.89 mm
Theoretical pitch for oscillation marks (speed/frequency):	8.01 mm
Superheat:	32 °C

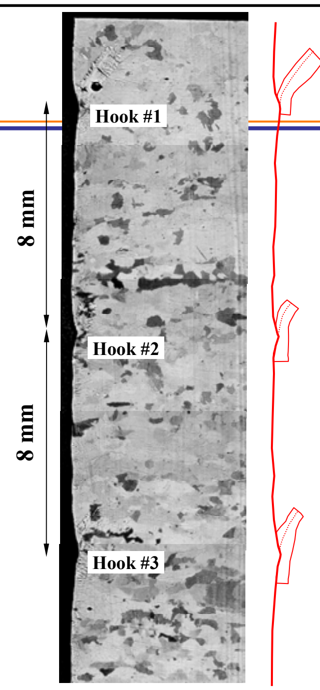

Objectives

I. Graphically track the positions of the following on a Cartesian space for one mold oscillation cycle:
Meniscus, mold, solid/liquid flux interface, shell, OM/Hook mark nos. 2 & 3

II. Using above positions and final morphology of the cast slab sample as templates, events leading to formation of OM & hook mark no. 1 will be identified

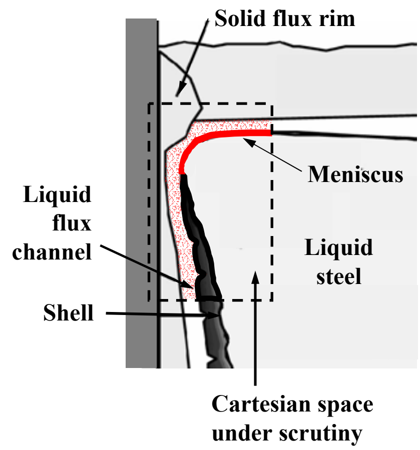

Equilibrium shape of meniscus

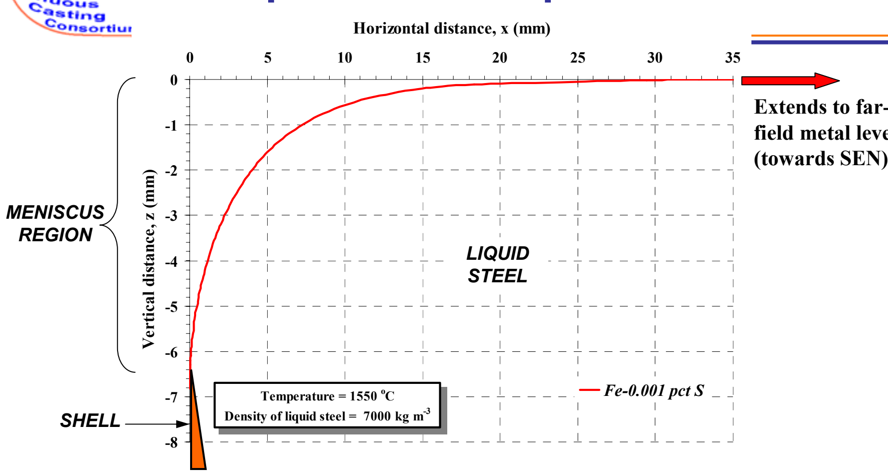

Assumptions: I. Far field metal level remains unpeturbed at all times (*z = 0 mm*)
II. *x = 0 mm* corresponds to mold wall
III. Dynamic effects active for x < 35 mm

Mold & shell velocity

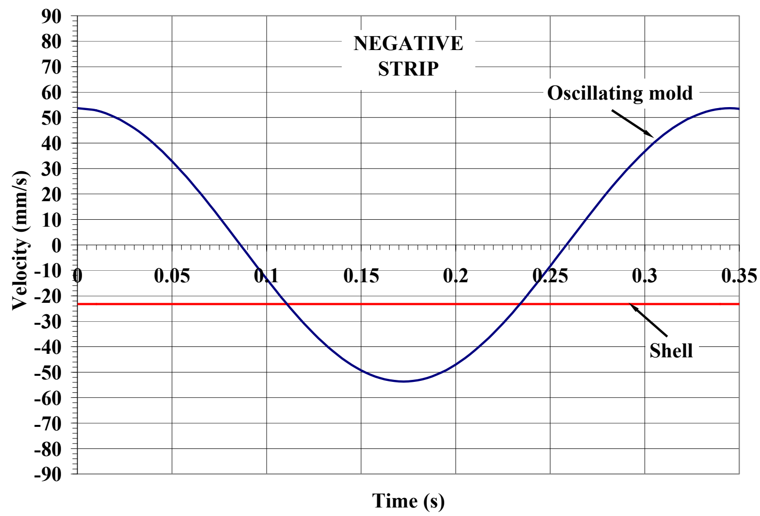

Mold position

Position corresponds to *z = 0 mm* & lines up with far-field metal level

At $t_{start} = 0$ *s*:

Position of OM #2:
6.4 + 8 = 12.4 mm

Position of OM #3:
12.4 + 8 = 20.4 mm

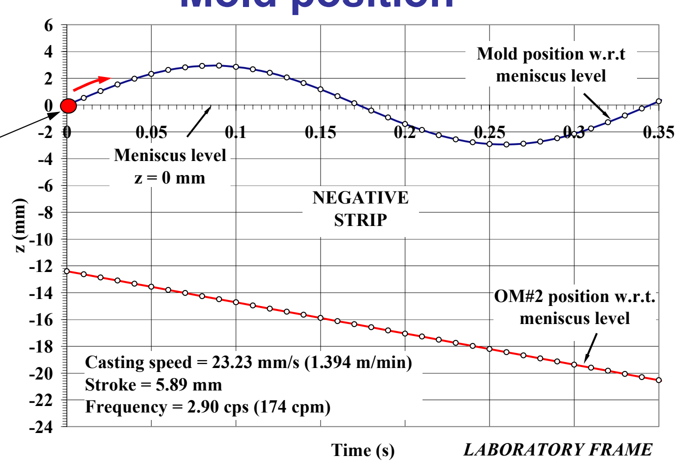

Meniscus shape is assumed to be in equilibrium at $t_{start} = 0$ *s*
- **Mold acceleration is zero → Inertia force is absent at this instant**
- **Positive flux pressure built-up during NST has been dissipated completely**
- **Hence, only surface tension forces will determine the shape of meniscus**

Profile of solid flux rim

- Profile of solid rim above the meniscus has been reported in literature, with:
  Solidus for steel = 1399 °C
  (actual 1517 °C)
  Solidus for slag = 1130 °C
  (actual 1180 °C)
  Superheat = 5 °C

- The shape has to be modified to correspond to actual superheat of 20 °C

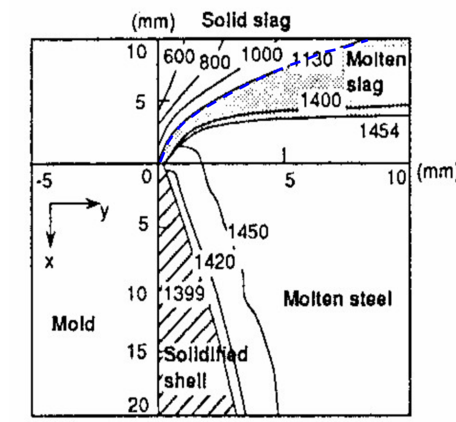

Takeuchi et al., 1983

Evolution of shell thickness predicted by CON1D

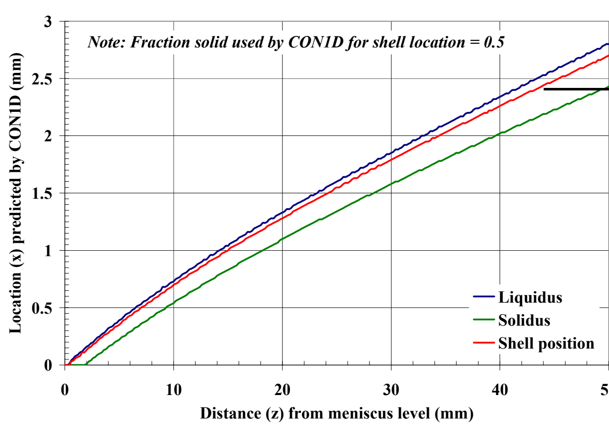

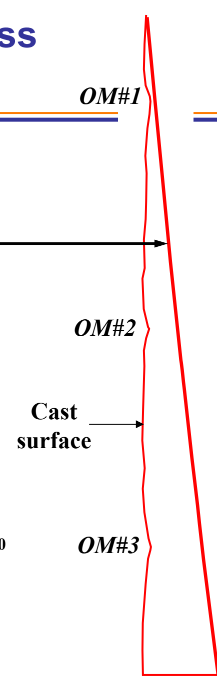

Reduction in shell thickness due to OM

OM area for OM nos. 1, 2 & 3:
(0.2 + 0.16 + 0.24)/0.236
= 2.54 mm^2/cm at ~20 mm below meniscus

Based on literature, about ~16% reduction in shell thickness should be observed at each oscillation mark.
(Actual for OM#3 = 17%)

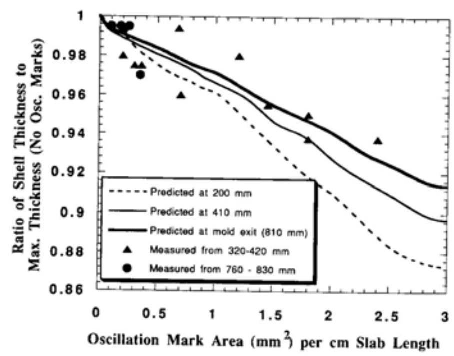

From B.G. Thomas et al., Sensors & Modeling in Mat. Processing, 1997

Summary of events in one oscillation cycle

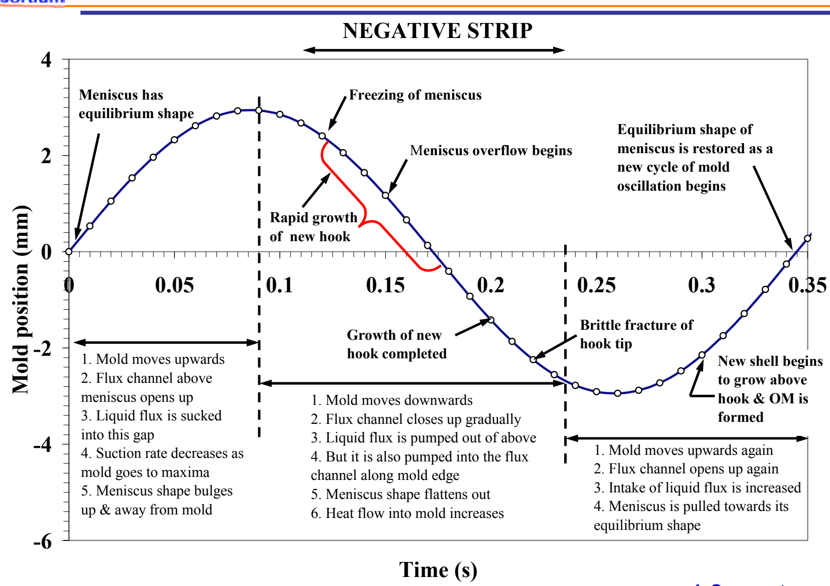

Experimental observations on a Sn-Pb alloy/stearic acid based casting simulator

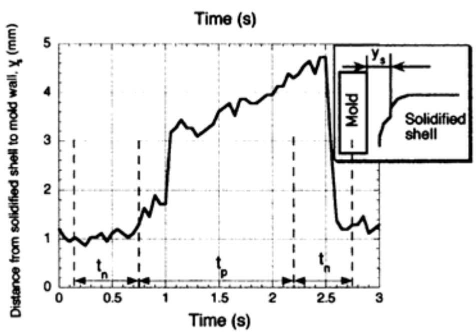

Sudden decrease in y_s during NST caused by liquid steel overflow over a hook & subsequent solidification

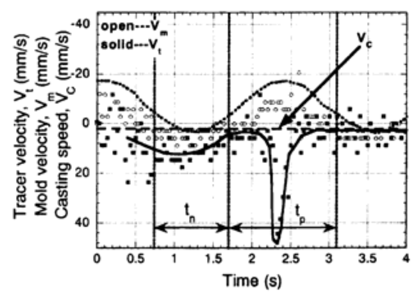

Sudden rise in tracer velocity during PST caused by creation of additional space in tracer channel due to OM formation

Tsutsumi et al., ISIJ International, 2000

Summary

I. A new mechanism of hook formation proposed based on:

- *Analysis of hook micrographs & EBSD images*
- *Meniscus shape predictions by Bikerman equation*
- *Prediction of distorted shell shapes by modifying CON2D*
- *Comparison of hook shapes with both meniscus shapes and distorted shell shapes*

  (Most hooks match best with meniscus shape)

Summary

II. Hook formation has been graphically animated & depicts:

- *Change of meniscus shape during one oscillation cycle*
- *Menicus freezing during negative strip period*
- *Overflow of liquid steel over curved hook (frozen meniscus) during negative strip period*
- *Hook formation & growth and subsequent fracture of tip*

III. The new mechanism can satisfactorily explain the formation of oscillation marks and hooks in ultra-low carbon steel slabs

However, shell distortion can still play an important role during oscillation mark formation in pertectic steels.

Shell distortions for different grades without any level fluctuation

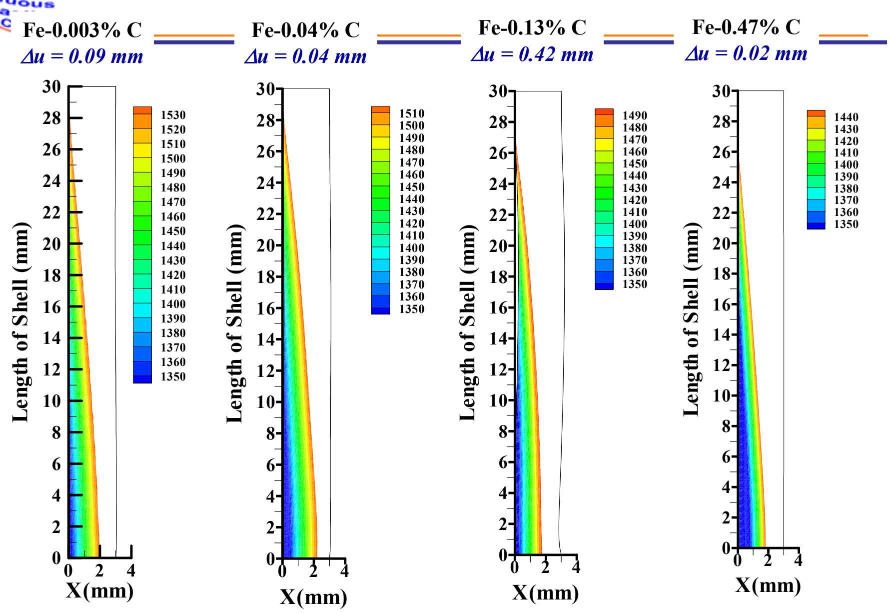

Acknowledgements

Continuous Casting Consortium
University of Illinois

Ho-Jung Shin & Go-Gi Lee
Graduate Students, POSTECH, South Korea
For hook samples and micrographs

POSCO, South Korea
For providing samples and data

Natural Sciences & Engineering Research Council
Canada